Supplementary Information

Perylene Diimide-based Electron Transport Layer Enabling Efficient Inverted Perovskite Solar Cells

Kui Jiang,[b†] Fei Wu,[*a†] Hui Yu,[a] Yanqing Yao, [a] Guangye Zhang,[b] Linna Zhu[*a] and He Yan[*b].

[a] Chongqing Key Laboratory for Advanced Materials and Technologies of Clean Energy, Faculty of Materials & Energy, Southwest University, Chongqing 400715, P.R.

[b] Department of Chemistry and Energy Institute, The Hong Kong University of Science and Technology, Clear Water Bay, Hong Kong.

*Email: hyan@ust.hk; feiwu610@swu.edu.cn; lnzhu@swu.edu.cn.

METHODS

Materials: In this work, all major materials were purchased from commercial suppliers and used without further purification, including P3CT (Rieke Metals), PbI_2 (*p*-OLED, >99.99 %), MAI (*p*-OLED, ≥99.5 %), PCBM (*p*-OLED, ≥99 %), C60 (*p*-OLED), BCP (*p*-OLED), Rhodamine 101 (Sigma-Aldrich), DMF (Sigma-Aldrich, 99.8 %), DMSO (Sigma-Aldrich, 99.8 %) and CB (Sigma-Aldrich, 99.8 %).

Device Fabrication: ITO-coated glass was sequentially washed by sonication using deionized water, ethanol and acetone. The hole transporting layer P3CT-Na was formed on ITO substrates by spin coating at 4000 rpm for 60 s followed by annealing at 140 °C for 30 min.[1] Then the samples were transferred into a N_2-filled glovebox. A $CH_3NH_3PbI_3$ precursor solution (1.4 M in DMF:DMSO mixed solution with a v/v of 4:1) was spin-coated in a two-step program at 400 and 5000 rpm for 3 and 30 s, respectively. During the second step, 200 μL of chlorobenzene was dropped on the spinning substrate at 10 s after the start-up. Next, the as-spun perovskite layer was annealed on a hot plate at 60 °C for 1 min and at 80 °C for 2 min to drive off solvent and form the perovskite phase. The thickness of perovskite layer measured by step profiler is about 345 nm. Then, PCBM or TPE-PDI_4 solutions in chlorobenzene were spin-coated onto the perovskite layer. To fabricate the ITO/P3CT-Na/Perovskite/ETL/Rhodamine 101/LiF/Ag device, Rhodamine 101 was deposited by spin coating Rhodamine 101 solution (0.05 wt% in isopropanol) at 1000 rpm for 40 s onto the ITO/P3CT-Na/Perovskite/ETL substrate.[2] Thus the thickness for Rhodamine 101 buffer layer is quite thin (less than 1 nm). Afterwards, 1 nm thick LiF was then thermally evaporated, and an approximately 100 nm thick Ag counter electrode was deposited on top to finish the device fabrication. The Rhodamine 101 and LiF layers are the double interlayers (buffer layer) between ETL and Ag electrode. To fabricate ITO/P3CT-Na/Perovskite/ETL/C60/BCP/Ag device, C60 (20 nm) and BCP (8 nm) were evaporated under

high vacuum on top of the ITO/P3CT-Na/Perovskite/ETL substrate. Finally, a 100 nm thick Ag electrode was deposited through a shadow mask. The active area of our device is 0.09 cm^2.

Device Analysis: UV-vis absorption spectra were measured on a Shimadzu UV-2450 absorption spectrophotometer. XRD was performed on a Japan Shimadzu XRD-7000 diffractometer. The morphology of perovskite films were characterized by FE-SEM images (JSM-7800F). AFM images were collected in air on a Bruker AFM using a tapping mode. The current–voltage (*J–V*) curves were measured under 100 mW cm^{-2} (AM 1.5 G) simulated sunlight using Keithley 2400 in conjunction with a Newport solar simulator (94043A). The external quantum efficiency (EQE) was calculated from the photocurrent measurement under monochromatic illuminations at different wavelengths, using a 150 W xenon lamp and a monochromator. Steady-state PL spectra were recorded on FS5 fluorescence spectrometer. Time-resolved PL decay curves were measured by a single photon counting spectrometer from Edinburgh Instruments (FS5). The impedance spectra were measured with CHI in the dark at a bias of 0.9 V.

Long-term Air Shelf Stability Test: Un-encapsulated devices were stored under dark condition and ambient or nitrogen atmosphere. The devices were measured under AM 1.5G one sun illumination (100 $mWcm^{-2}$) until 400 h storage. The relative humidity was in the range 35-40%, and temperature was 25±3 ^oC. After each measurement test, the devices were stored back under dark.

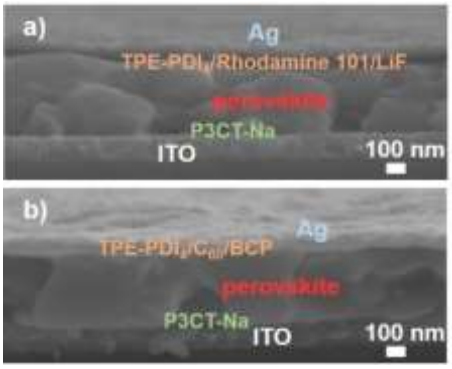

Figure S1. Cross-sectional SEM images of devices with (a) ITO/P3CT-Na/Perovskite/TPE-PDI_4/Rhodamine 101/LiF/Ag and (b) ITO/P3CT-Na/Perovskite/TPE-PDI_4/C_{60}/BCP/Ag configuration.

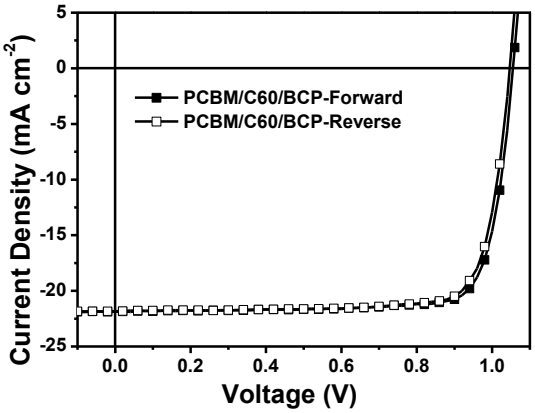

Figure S2. Forward and reverse scan of inverted PSCs based on PCBM interlayer.

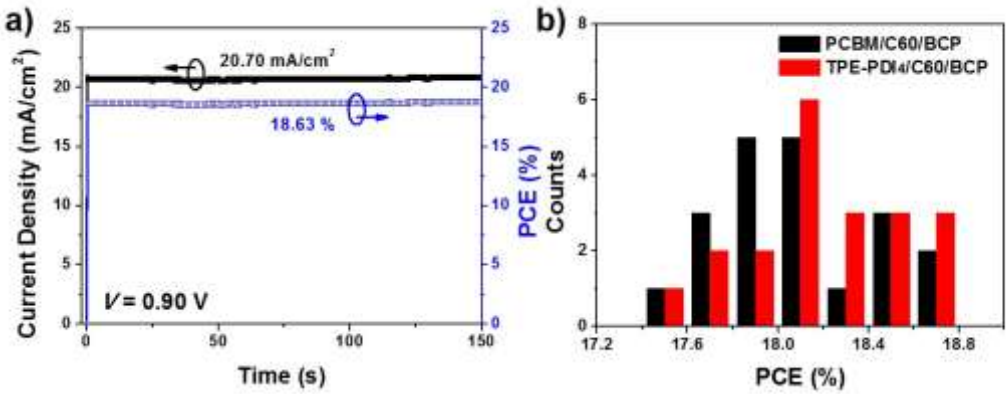

Figure S3. a) Stabilized photocurrent density and efficiency output of TPE-PDI_4 interlayer-based device; b) PCE distributions based on 20 devices.

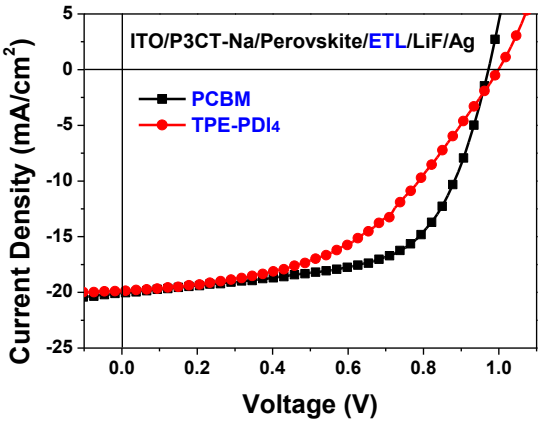

Figure S4. *J-V* curves of TPE-PDI$_4$ or PCBM as electron transport material in inverted PSCs without the Rhodamine 101 buffer layer.

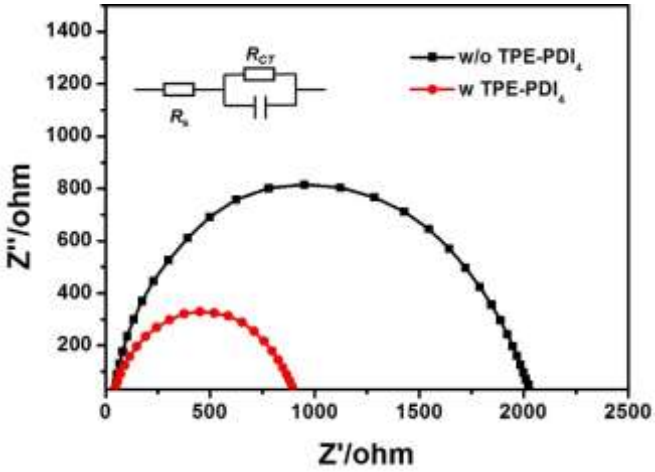

Figure S5. Nyquist plots of the inverted PSCs with and without TPE-PDI4 interlayer measured in the dark condition. Inset shows the equivalent circuit model for the PSCs studied.

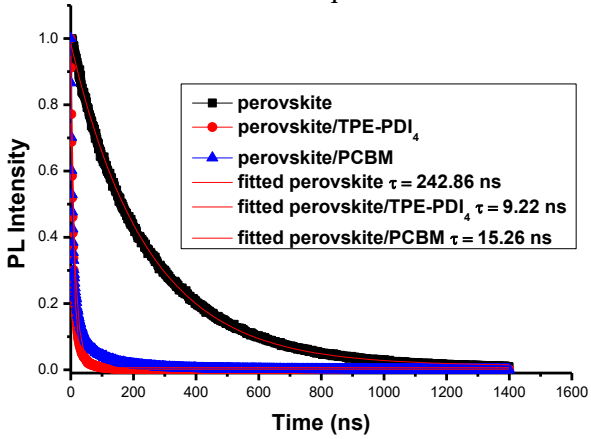

Figure S6. Fitted PL decay of perovskite, perovskite/TPE-PDI$_4$ and perovskite/PCBM.

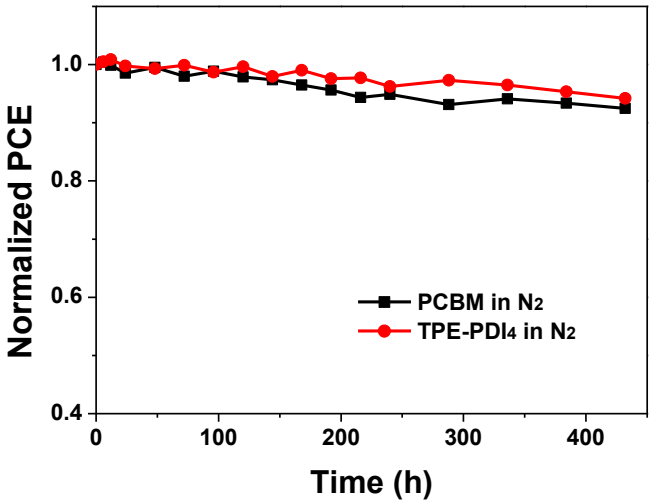

Figure S7. Stability test of the devices in N_2 atmosphere with TPE-PDI_4 or PCBM as the electron transporting material.

Table S1. Summary of the photovoltaic performances of PSCs with TPE-PDI_4 ETL in different thicknesses. PCBM is for comparison.

Device	V_{oc} (mV)	J_{sc} (mA cm^2)	*FF*	PCE (%)
TPE-PDI_4 (45 nm)	983	21.13	0.71	14.67
TPE-PDI_4 (37 nm)	1013	21.68	0.74	16.29
TPE-PDI_4 (19 nm)	885	19.36	0.67	11.54
TPE-PDI_4 (12 nm)	846	18.76	0.56	8.85
TPE-PDI_4 (5 nm)	293	15.33	0.39	1.73
PCBM	1022	20.60	0.73	15.27

Table S2. Forward and reverse scan of PSCs using TPE-PDI_4 or PCBM as ETL.

Device	V_{oc} (mV)	J_{sc} (mA cm^2)	*FF*	PCE (%)
TPE-PDI_4 (forward)	1013	21.68	0.74	16.29
TPE-PDI_4 (reverse)	1006	21.67	0.74	16.10
PCBM (forward)	1022	20.60	0.73	15.27
PCBM (reverse)	1019	20.58	0.72	15.12

Table S3. Summary of the photovoltaic performances of PSCs with TPE-PDI$_4$ interlayer in different thicknesses. PCBM is for comparison.

Device	V_{oc} (mV)	J_{sc} (mA cm^2)	*FF*	PCE (%)
none	1038	21.01	0.76	16.56
TPE-PDI$_4$ (12 nm)	1023	20.71	0.72	15.26
TPE-PDI$_4$ (5 nm)	1052	21.98	0.81	18.78
TPE-PDI$_4$ (2 nm)	1046	21.20	0.80	17.71
PCBM	1055	21.87	0.81	18.77

Table S4. Forward and reverse scan of PSCs using TPE-PDI$_4$ or PCBM interlayer.

Device	V_{oc} (mV)	J_{sc} (mA cm^2)	*FF*	PCE (%)
TPE-PDI$_4$ (forward)	1052	21.98	0.81	18.78
TPE-PDI$_4$ (reverse)	1043	21.96	0.81	18.58
PCBM (forward)	1055	21.87	0.81	18.77
PCBM (reverse)	1046	21.82	0.81	18.44

Table S5. Summary of perylene diimide-based ETL in perovskite solar cells

ETLs	PCE	References
***t*-BPTI/PDI-C4 ETL**	10 %	ChemSusChem, 2018, 11, 415.[3]
PV-PDI	10.14 %	ACS Appl. Mater. Interfaces 2017, 9, 10983.[4]
Br-PDI	10.5 %	J. Mater. Chem. A, 2017, 5, 12811.[5]
SFX-PDI4	15.3 %	Sol. RRL 2017, 1, 1700046.[6]
PDI	11 %	Solar Energy Mater & Solar Cells 2017, 169, 78.[7]
hPDI3-Pyr-hPDI3	16.5 %	Angew. Chem. Int. Ed. 2017, 56, 14648-14652.[8]

SI REFERENCES

(1) X. Li.; X. Liu.; X. Wang.; L. Zhao.; T. Jiu.; J. Fang. Polyelectrolyte based hole-transporting materials for high performance solution processed planar perovskite solar cells. *J. Mater. Chem. A* **2015**, *3*, 15024.

(2) K. Sun.; J. Chang.; F. H. Isikgor.; P. Li.; J. Ouyang. Efficiency enhancement of planar perovskite solar cells by adding zwitterion/LiF double interlayers for electron collection. *Nanoscale*, **2015**, *7*, 896.

(3) P. Karuppuswamy, H.-C. Chen, P.-C. Wang, C.-P. Hsu, K.-T. Wong, and C.-W. Chu, *ChemSusChem*, 2018, **11**, 415.

(4) Q. Guo, Y. Xu, B. Xiao, B. Zhang, E. Zhou, F. Wang, Y. Bai, T. Hayat, A. Alsaedi, Z. Tan, ACS Appl. Mater. Interfaces, 2017, 9, 10983.

(5) J.-L. Wu, W.-K. Huang, Y.-C. Chang, B.-C. Tsai, Y.-C. Hsiao, C.-Y. Chang, C.-T. Chen, and C.-T. Chen, J. Mater. Chem. A, 2017, 5, 12811.

(6) M. Cheng, Y. Li, P. Liu, F. Zhang, A. Hajian, H. Wang, J. Li, L. Wang, L. Kloo, X. Yang and L. Sun, Sol. RRL, 2017, 1, 1700046.

(7) P. Karuppuswamy, C. Hanmandlu, K. M. Boopathi, P. Perumal, C.-C. Liu, Y.-F. Chen, Y.-C. Chang, P.-C. Wang, C.-S. Lai and C.-W. Chu, Solar Energy Mater & Solar Cells, 2017, 169, 78.

(8) E. Castro, T. J. Sisto, E. L. Romero, F. Liu, S. R. Peurifoy, J. Wang, X. Zhang, C. Nuckolls, L. Echegoyen, Angew. Chem. Int. Ed. 2017, 56, 14648.